

Sensors & Diagnostics

Accepted Manuscript

This article can be cited before page numbers have been issued, to do this please use: I. Ishika, W. M. Hassen, R. St-Onge, H. Moteshareie, A. Tayabali and J. J. Dubowski, *Sens. Diagn.*, 2024, DOI: 10.1039/D4SD00367E.



This is an Accepted Manuscript, which has been through the Royal Society of Chemistry peer review process and has been accepted for publication.

Accepted Manuscripts are published online shortly after acceptance, before technical editing, formatting and proof reading. Using this free service, authors can make their results available to the community, in citable form, before we publish the edited article. We will replace this Accepted Manuscript with the edited and formatted Advance Article as soon as it is available.

You can find more information about Accepted Manuscripts in the [Information for Authors](#).

Please note that technical editing may introduce minor changes to the text and/or graphics, which may alter content. The journal's standard [Terms & Conditions](#) and the [Ethical guidelines](#) still apply. In no event shall the Royal Society of Chemistry be held responsible for any errors or omissions in this Accepted Manuscript or any consequences arising from the use of any information it contains.

ARTICLE

Regenerable photonic aptasensor for detection of bacterial spores with stacks of GaAs-AlGaAs nanoheterostructures

Ishika Ishika^a, Walid M. Hassen^a, René St-Onge^a, Houman Moteshareie^{a,b}, Azam F. Tayabali^{a,b}, Jan J. Dubowski^{*a}Received 00th December 2024,
Accepted 00th January 20xx

DOI: 10.1039/x0xx00000x

The reusability of biosensors is a crucial advancement in environmental monitoring and laboratory efficiency. In this study, we introduce the concept of a regenerable aptasensor based on digital photocorrosion (DIP) of a GaAs-AlGaAs biochip, designed with alternating nanolayers of GaAs (12 nm) and AlGaAs (10 nm). Each GaAs-AlGaAs bilayer acts as an independent sensing unit. By employing a specific thiolated aptamer, we achieve efficient detection of *Bacillus thuringiensis* spp. *kurstaki* spores. The interaction between the thiolated aptamers with the targeted spores leads to the formation of aptamer-spore hybrids, which bind to the GaAs surface. The GaAs-AlGaAs nanoheterostructure biochip supports multiple biosensing cycles. After consumption of the first GaAs-AlGaAs bilayer, a simple regeneration step a high ionic strength buffer releases the bound spores and prepares subsequent nanolayers of the same biochip for reuse. The capability to regenerate and reuse individual nanolayers presents a novel and practical solution for reducing biosensor waste while improving operational efficiency. We further explore the conditions necessary for sustainable DIP operation in biochips containing multiple GaAs-AlGaAs nanolayer pairs, ensuring reliable performance over numerous biosensing cycles. Our findings establish a cost-effective and durable biosensing platform. These work marks a significant step toward quasi-autonomous biosensing technologies, paving the way for cost-effective and robust, reusable biosensors suitable for remote and field applications.

1. Introduction

Typical biosensors consist of three main components: a biorecognition element (bioreceptor), a transducer, and a signal-processing device¹. When a biomolecular target interacts with the biorecognition element, a quantifiable physical signal variation is measured and compared to the reference. Key attributes of an ideal biosensor include cost-effectiveness, user friendliness defined by operational readiness and portability, or even the ability to operate semi-autonomously in out of laboratory settings. The reusability of a biosensor is particularly important for devices designed for remote environmental sensing and monitoring. This requires either a regeneration procedure to overcome bioreceptor-analyte binding forces or washing of the biosensor followed by a re-functionalization procedure.

Chemical regeneration, achieved by submerging a transducer in a regeneration buffer, is the most frequently applied method. This method often involves acids/bases, low concentration

detergents, and high ionic strength solutions². For instance, a relatively inexpensive regeneration method demonstrated a five-fold regeneration of a ZnO/bulk GaAs acousto-optic biosensor for detection of *Escherichia coli*³. The use of a pH 2 buffer can break antibody-antigen binding, while high ionic content can eliminate aptamer-target interaction⁴. Heating 2% sodium dodecyl sulfate (SDS) at 50 °C enabled the regeneration of a fluorescence biosensor with a cyclodextrins-mannose entity designed to capture *E. coli*⁵ whereas heating at 80 °C was used for regenerating an aptamer-based impedimetric biosensor of *E. coli*⁶. Up to seven regeneration steps were demonstrated with a surface plasmon resonance (SPR) biosensor designed for detecting small molecules, such as ochratoxin A⁷. However, the sensitivity of SPR biosensors is typically limited by the penetration depth of evanescent waves, which does not exceed a few tens of nm⁸. This results in relatively poor responses to large bio-objects, such as bacteria⁹. Additionally, sensitive SPR devices are relatively bulky and prohibitively expensive. Fiber optic-based biosensors also suffer from the high cost of the reading equipment. Regenerable configuration of fluorescence⁵, quartz crystal balance¹⁰, acoustic wave³ and electrochemical^{11, 12} biosensors have been reported for detecting bacteria. However, common challenges include bulky equipment³, the risk of damaging recognition elements¹¹, and the loss of sensitivity^{5, 10, 12}. These issues could be related to the deterioration of the quality of sensing surface, such as gold in SPR biosensors⁷, or the denaturation of recognition linkers¹¹. Examples of biosensors investigated for their regeneration characteristics are listed in Table S1 (Supplementary Information).

^a Interdisciplinary Institute for Technological Innovation (3IT), CNRS IRL-3463, Quantum Semiconductors and Photon-based BioNanotechnology Group, Department of Electrical and Computer Engineering, Université de Sherbrooke, 3000, boul. de l'Université, Sherbrooke, Québec J1K 0A5, Canada.

^b Biotechnology Laboratory, Environmental Health Science and Research Bureau, Healthy Environments and Consumer Safety Branch, Health Canada, 251 Sir Frederick Banting Driveway, Ottawa, Ontario, K1A 0K9, Canada.

*Address correspondence to

Jan.J.Dubowski@usherbrooke.ca (submitting author)

† Supplementary Information available: [details of any supplementary information available should be included here]. See DOI: 10.1039/x0xx00000x



Our interest concerns detection of *Bacillus cereus* (*Bc*) - a foodborne pathogen¹³ with its infectious dose at 10^3 CFU/mL¹⁴,¹⁵, and *Bacillus anthracis* (*Ba*) known for its use as a biological weapon¹⁶. In that context, we investigated detection of *B. thuringiensis* to act as a surrogate for *Ba* and *Bc*, based on the high similarity of spore structures among members of the *Bacillus cereus* Group¹⁹. Although there are a few reports of *Bt* toxicity in humans, distinguishing between *Bt* and *Bc* is challenging, leading to an underestimation of *Bt*'s real impact, particularly in relation to enterotoxins¹⁷.

Detection of *B. anthracis* toxin was demonstrated with aptamer-based electrochemical biosensor¹⁸. However, the detection of toxins requires sample processing that may not ensure rapid and cost-effective pathogen detection compared to identifying whole bacteria¹⁹. Also, it may provide limited information of the infection as there could be many bacterial species producing structurally and functionally similar toxins²⁰. Biosensors based on digital photocorrosion (DIP) of GaAs-AlGaAs nanoheterostructures have recently been introduced for detecting bacteria and spores²¹⁻²⁷. The operation of the DIP biosensor is based on the controlled photocorrosion of GaAs-AlGaAs nanoheterostructures, which is monitored via the photoluminescence (PL) signal originating from GaAs^{28, 29}. The DIP process is highly sensitive to the presence of charged molecules/macromolecules/bacteria in the vicinity of the chip surface. The distinct surface recombination rates of GaAs and AlGaAs²⁹ result in the formation of a PL intensity maximum (PL_{max}) when the photocorrosion front reaches the interface of a ~20 nm thick GaAs-AlGaAs nanolayer pair. The timing of the PL_{max} appearance is influenced by charge transfer interactions between the biochip and detected target, allowing for precise calibration of bacterial concentrations. This approach has been successfully demonstrated for the detection of *Legionella pneumophila*^{22, 23, 25} and *E. coli*²¹, and was recently applied to aptamer-based spore detection²⁷. Up-to-date DIP biosensing results have been based on recording GaAs PL signal originating from a single pair of GaAs (12 nm)-AlGaAs (10 nm) nanolayers. Given that a series of PL_{max} can be produced by DIP of a series of GaAs-AlGaAs nanolayers^{28, 30}, we hypothesized that each pair of GaAs-AlGaAs nanolayers could be employed for repetitive biosensing with the same biochip. Here we discuss this concept and present the results of repetitive detection of *Bacillus thuringiensis kurstaki* (*Btk*) spores.

This work represents a significant advancement in biosensor technology by integrating nanoscale heterostructures with aptamer-based recognition for highly specific and repetitive detection of spores. The innovative concept of utilizing multiple GaAs-AlGaAs nanolayer pairs within a single biochip for sequential biosensing cycles not only extends the operational lifespan of the sensor but also reduces material consumption, improving cost-efficiency. By applying the DIP methodology for *Btk* spore detection, this study broadens the scope of autonomous biosensing to include reusable platforms, an essential step toward practical, field-deployable solutions.

2. Experimental methods

2.1 Materials and Reagents

Semiconductor grade acetone was purchased from Allied and Chemical Products Inc. (ACP, Montréal, Canada). OptiClear was sourced from National Diagnostics (Mississauga, Canada), and isopropanol was obtained from Fisher Scientific (Ottawa, Canada). The 28% ammonium hydroxide (NH_4OH) was provided by Anachemia (Richmond, Canada) and used without further purification. The anhydrous ethanol from Commercial Alcohols, Inc. (Brampton, Canada), was degassed by flushing with high-purity nitrogen gas (99.9995%) that was obtained from Praxair, Canada. 11-mercapto-1-undecanol (MUDO) thiol and phosphate buffered saline (PBS) solution (10X, pH 7.4) were purchased from Sigma-Aldrich (Oakville, Canada). *Bacillus thuringiensis kurstaki* (strain HD1) was drawn from the Foray 48B. Thiolated aptamers (Apt) against *Btk* spores were obtained from IDT (Ontario, Canada). The deionized (DI) water with a resistivity of 18.2 M Ω was produced by a customized Millipore purification system assembled by Culligan (Québec, Canada). The GaAs-AlGaAs wafer, obtained through CMC Microsystems (Ottawa, Ontario, Canada), comprised a stack of 7 bilayers of GaAs (12 nm) - $Al_{0.35}Ga_{0.65}As$ (10 nm). The first two pairs of these bilayers were investigated for repetitive biosensing.

2.2 Chip preparation

2 mm \times 2 mm chips were cut out from a GaAs-AlGaAs wafer (D3422) using a high-precision diamond saw (DAD 320, Disco). The chips were sequentially cleaned with acetone, OptiClear, acetone again, and isopropanol (IPA), with each step performed for 5 minutes under sonication. Native oxides were removed from the chips by etching in 28% ammonium hydroxide (NH_4OH) solution for 2 minutes, followed by a quick rinse with degassed ethanol. Immediately after, the chips were immersed in 1 mM 11-mercapto-1-undecanol (MUDO) thiol solution in degassed ethanol for 20 hours. The chips were then sonicated for 1 minute, rinsed with degassed ethanol to remove the unbound thiols, and dried using high-purity nitrogen gas. This results in the immobilization of thiols on the chip surface, which is tilted at approximately 19°, due to hydrophobic interactions³¹. MUDO thiols form a self-assembled monolayer (SAM) on the GaAs surface, which partially passivates to the chip surface. By engaging the sulphur bond of thiols with GaAs atoms, thereby decreasing the photocorrosion rate²¹. The resulting decrease in DIP leads to a desirable resolution of PL_{max} plots and accurate detection of spores. Aptamers against *Btk* spores were premixed with spores at concentrations of 10^3 , 10^4 , and 10^5 CFU/mL and incubated for 1 hour at room temperature to form spore-aptamer hybrids. The MUDO thiolated chips were incubated in these suspensions for 1 hour and then washed three times with 1X PBS. Aptamers at 5 μ M/mL were premixed with spores at concentrations of 10^3 , 10^4 , and 10^5 CFU/mL and incubated for 1 hour at room temperature to form spore-aptamer hybrids. Following that, MUDO thiolated chips were incubated in each of the prepared spore-aptamer suspensions for 1 hour and washed three times with PBS. Reference chips were prepared by incubating MUDO thiolated chips in pure 5 μ M thiolated aptamers in 1X PBS, followed by washing three times with PBS. Figure 1 schematically illustrates the formation



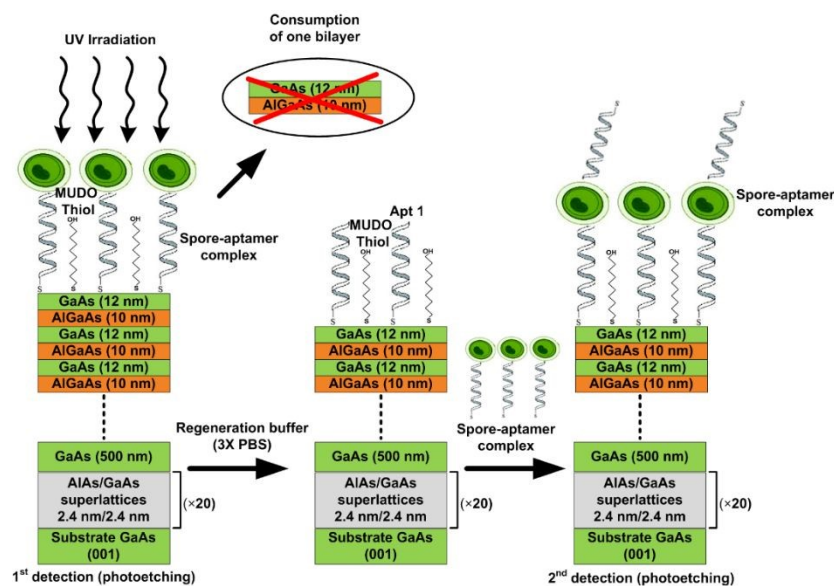


Figure 2. Schematic illustration of a GaAs-AlGaAs biochip designed to detect *Btk* spores by sequential DIP of GaAs-AlGaAs nanolayers.

2.4 PL monitored DIP process

Detection and reference runs were conducted using a custom-designed quantum semiconductor photonic biosensing (QSPB-3) reader³². The chips were irradiated with a 375 nm LED, and PL emission from GaAs (maximum intensity at 870 nm) was collected with a CCD camera²². Experiments were conducted with intermittent 1.5-second irradiation at power density of 15 mW/cm², separated by 5-sec dark phase. Functionalized biochips underwent DIP under continuous flow of 1X PBS at 100 μ L/min. The schematic diagram of the physical prototype of our DIP biosensor is presented as Figure S1 in the Supplementary Information section. For repetitive detection, after revealing the first PL intensity peak, the DIP process was stopped at the intermediate PL intensity minimum, and the spores were released using the aptamer regeneration buffer. Reference chips were also exposed to the regeneration buffer for the same duration. Afterwards, the reference and detection chips were incubated in aptamer solution and aptamer-spore hybrids, respectively, for 1 hour, followed by washing with 1X PBS before conducting the second series of DIP cycle.

The effect of UV irradiation (375 nm) on aptamer reactivity was evaluated by exposing a 20 μ L drop of 100 μ M aptamer solution to UV light for 5 minutes. The UV-treated aptamer was then tested for spore capture at 10⁵ *Btk* spores/ml. Spore immobilization was quantified using optical microscopy and compared to results obtained from non-UV-treated aptamers. Blind tests were performed with biochips exposed sequentially to two suspensions of spores at unknown concentrations (UC1 and UC2) determined by the first and second GaAs-AlGaAs bilayer.

3. Results

3.1 Validation of the regeneration efficiency

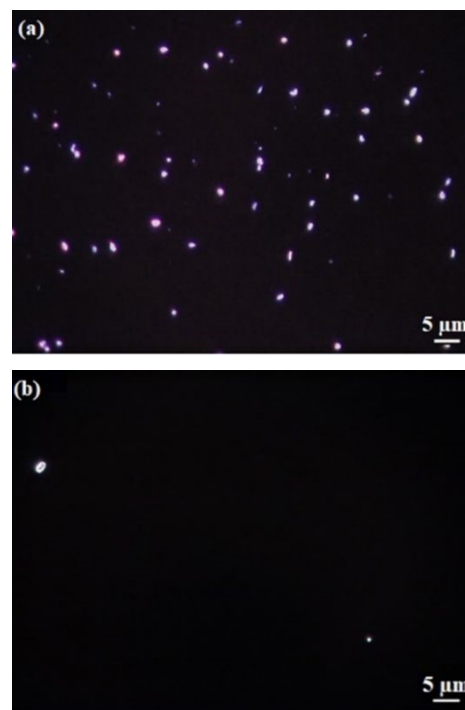


Figure 3. Optical microscope images of MUDO functionalized GaAs chips exposed to Apt-*Btk* hybrids at 10⁵ CFU/mL (a), and after regeneration involving submersion in 3X PBS for 20 minutes (b).

The efficiency of releasing the spores by an aptasensor submerged in PBS buffer solution is illustrated with examples of optical microscopic images shown in Figure 3. The MUDO



functionalized GaAs chip exposed to Apt-*Btk* hybrids at 10^5 spores/mL shows an average 1920 ± 108 spores/mm² (Fig. 3a), which is compared to 115 ± 30 spores/mm² for the chip exposed for 20-min to 3X PBS (Fig. 3b). Thus, this regeneration procedure corresponds to the 94% efficiency of removing *Btk* spores.

3.2 Repetitive detection of *Btk* spores using GaAs-AlGaAs DIP aptasensor

Temporal PL intensity plots collected during DIP of two consecutive pairs of GaAs-AlGaAs nanolayers are shown in Figure 4. Increasing spore concentration accelerated the formation of PL intensity maxima observed with the first and second pairs of GaAs-AlGaAs nanolayers. The statistical error of 45 samples, summarized in Figure 5, revealed PL_{max} value for the first pair of GaAs-AlGaAs nanolayers at 48.6 ± 1.3 min, 37.1 ± 0.9 min, 27.3 ± 0.9 min, and 18 ± 0.5 min for the reference run and spore suspensions at 10^3 , 10^4 , and 10^5 CFU/mL, respectively. For the second pair of GaAs-AlGaAs nanolayers, PL_{max}

values were 40.9 ± 2.1 min, 33.1 ± 1.6 min, 24.5 ± 2.2 min, and 15 ± 2.1 min, respectively, for nominally the same experimental conditions. These findings are further detailed in Table S2 (Supplementary information).

The binding ability of the aptamer was not affected by UV irradiation. The observed spore immobilization was at 1735 ± 138 *Btk* spores/mm² for UV-treated aptamers, compared to 1920 ± 108 *Btk* spores/mm² for non-UV-treated aptamers. The variation between these conditions is statistically insignificant as shown in Figure S2. Calibration plots derived from DIP using the first and second pairs of GaAs-AlGaAs nanolayers were employed for blind tests with two unknown concentrations (UC) as illustrates Figure 6. Experimental points (triangle up and down) show detection of *Btk* spores at 1.6×10^4 CFU/mL (UC1) and 4×10^3 CFU/mL (UC2). These results compare to the intended spore concentrations of 2×10^4 CFU/mL and 5×10^3 CFU/mL, respectively, indicating an error not exceeding 20%.

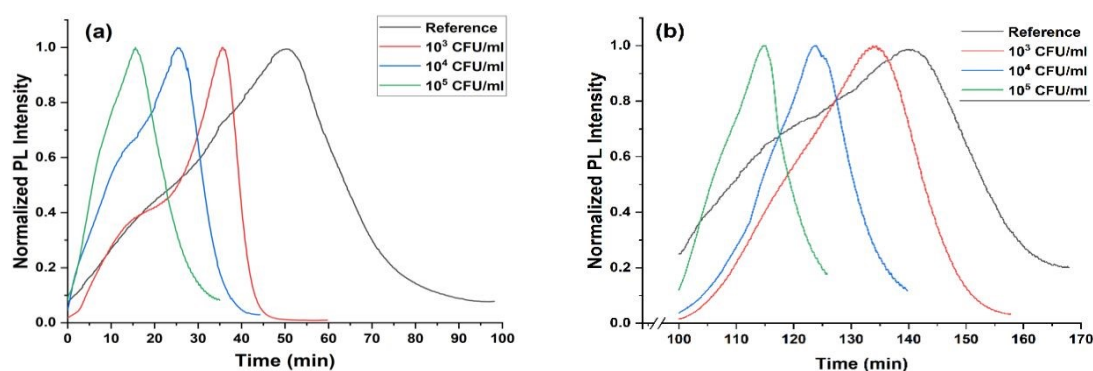


Figure 4. Examples of PL intensity plots collected for the first (a) and second (b) pairs of GaAs-AlGaAs nanolayers of the regenerable DIP aptasensor.

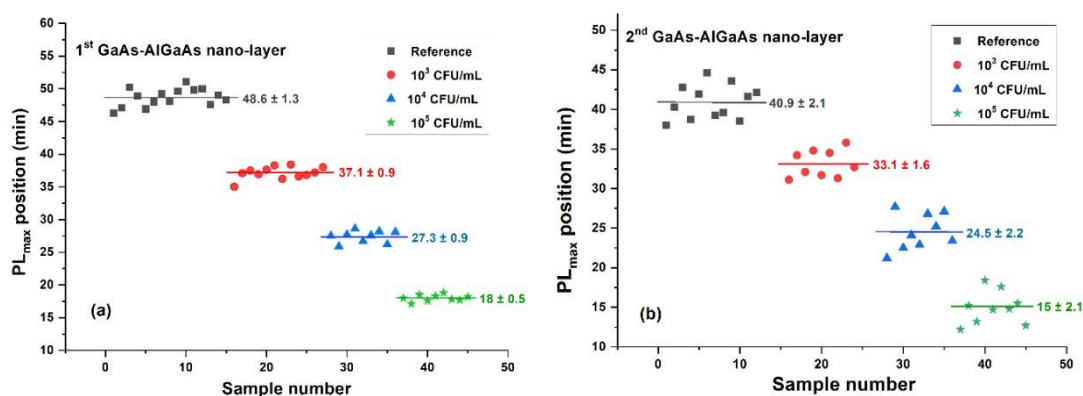


Figure 5. Examples of PL intensity plots collected for the first (a) and second (b) pairs of GaAs-AlGaAs nanolayers of the regenerable DIP aptasensor.



We note that detection errors of bacteria achieved with relatively advanced technologies, such as fluorescence-based biosensing reported the related errors ranging between 5 and 23 %, respectively, by Li et. al.,³³ and Chattopadhyay et. al.,³⁴. Thus, our approach offers attractive results in that context and while taking the relatively early stage of development of the undelaying technology.

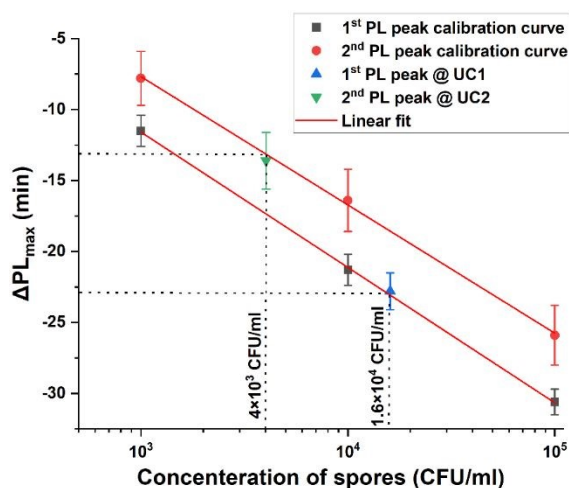


Figure 6. Calibration plots of ΔPL_{max} determined with respect to the reference runs for the first (black square) and second (red circle) pairs of GaAs-AlGaAs nanolayers. Experimental points corresponding to blind tests determined with the first (blue triangle) and second (green inverted triangle) nanolayers.

Negative control experiments were conducted using non-*Bc* group spores (*Bm*). The PL maximum for *Bm*-aptamer hybrid is observed at 45.9 ± 2.7 min, overlapping with the reference PL maximum at 48.6 ± 1.3 min. This result confirms the specificity of the aptamer used, and consequently, the reliability of our biosensing method (Figure S3, Supplementary Information). Optical microscopy imaging of GaAs chips exposed to the *Bm* spore-aptamer hybrid showed that captured spore densities did not exceed 277.6 ± 48 spores/mm². This was 7 times lower than what was obtained for our target *Btk* spores (1920 ± 108 spores/mm²) under the same tested concentration of 10^5 spores/ml.

The successful detection of *Btk* spores in Mago River water is demonstrated in Figure S4 (Supplementary Information). The results indicate that the presence of *Btk* spores significantly accelerated the temporal position of the PL peak, shifting from 71.2 ± 2.3 min to 48.3 ± 3.3 min in the first bilayer and from 57.5 ± 3.1 min to 35.8 ± 3.8 min in the second bilayer. These findings align with the previously observed results under controlled laboratory conditions, further supporting the practical applicability of our biosensor.

4. Discussion

The immobilization of thiolated aptamer-spore hybrids on the GaAs-AlGaAs biochip induced charge exchange between the biochip and the semiconductor surface. The loss of electrons by the semiconductor biochip accelerates photocorrosion in proportion to the density of immobilized spores, which is facilitated by the relatively short length (~3 nm) of the aptamer linker³⁵. The proximity

of spores to the biochip surface is important characteristics of a DIP GaAs-AlGaAs biosensor. Attempts to develop a similar device using antibody-functionalized GaAs-AlGaAs biochips were less successful, likely due to the significantly greater antigen-biochip surface distance (~15 nm), resulting in excessively reduced photocorrosion rates and wider PL_{max} features²⁵.

The increased error in PL_{max} determination for the second pair of GaAs-AlGaAs nanolayers (Fig. 5) is attributed primarily to surface roughness changes resulted from DIP. While some residual spores might contribute to this effect, the primarily cause must be related to the quality of DIP-produced surface. The principal source of the increased roughness are Ga oxides that, normally, require processing with ammonia but accumulate on the surface of biochips photocorroding in PBS environment. This is in addition to Al-based products that accumulate even in an ammonia environment. A comparison of the atomic force microscopy surface roughness (σ_{RMS}) of GaAs-AlGaAs biochips functionalized with MUDO and aptamer showed the increase of σ_{RMS} from 0.81 nm to 1.32 nm and 2.12 nm after DIP of, respectively, first and second pair of GaAs-AlGaAs nanolayers (Figure S5, Supplementary information). An independent research of the similar GaAs-AlGaAs biochip functionalized with a 16-mercaptohexadecanoic acid self-assembled monolayer revealed σ_{RMS} increased from the initial 0.5 nm to 1.9 nm after DIP of the second pair GaAs-AlGaAs of nanolayers³². Accurate determining PL_{max} positions is important to the measurable differentiation of results originating from suspensions with different concentrations of spores, and to the development of regenerable DIP biosensors.

The specificity of our DIP aptasensor was further confirmed by the negligible variation in the PL maximum temporal position for *Bm* compared to the reference. This finding aligns with previous data reported by Houman et al.¹⁹, demonstrating that the aptamer used in this study exhibits significantly higher capture efficiency for *Btk* spores compared to *Bm* or *B. subtilis* spores.

The presence of impurities in the Mago River water influenced the temporal position of the PL intensity maxima, leading to a delay in the photocorrosion rate for both reference and detection samples compared to the pristine conditions. This delay may be attributed to the presence of ionic species in Mago River water sample. However, this effect did not compromise the ability of our biosensor to detect *Btk* spores, demonstrating its robustness and applicability for environmental monitoring.

Clearly, sustainable DIP of devices with numerous pairs of GaAs-AlGaAs nanolayers is crucial to operation of biochips capable of delivering a large number of biosensing runs³⁶. Given that neither water nor PBS environments support photoetching of Al-based products, this requires development of a dedicated chemical processing protocol.

5. Conclusions

This study demonstrated the functionality of a regenerable DIP biosensor incorporating two pairs of GaAs (12 nm) - AlGaAs (10 nm) nanolayers. The biochip surface was coated with low-density MUDO SAM, designed to reduce DIP rates and enable attractive detection of *Btk* spores at concentrations between 10^3 - 10^5 CFU/mL. An



enhanced limit of detection is still possible with this method, e.g., by pre-concentrating spores in tested water samples.

The application of thiolated aptamers, specific to *Btk* spores, facilitated the immobilization of spore-aptamer hybrids on the biochip surface. After completing the biosensing run with the first pair of nanolayers, exposure to 3X PBS released the spores, and prepared the same biochip for another run with the second pair of nanolayers.

The regenerable biosensor was blind tested for detection of *Btk* spores in samples spiked at 2×10^4 CFU/mL and 5×10^3 CFU/mL. The results reveal the protocol of a repetitive detection involving the same GaAs-AlGaAs biochip with an error not exceeding 20%, i.e., comparable to such errors reported with by other biosensing technologies. We argue that a chip with stacks of numerous pairs of GaAs-AlGaAs nanolayers, the production of which is readily available with the current semiconductor manufacturing technology, can deliver a large amount of biosensing data before getting swapped with a new unit. This should be of high interest to the development of biosensing workstations for quasi-continuous operation in out-of-laboratory settings attractive for environmental monitoring.

Author contributions

Conceptualization, methodology, writing original draft: Ishika Ishika, Walid M. Hassen. Formal analysis and investigation: Ishika Ishika, Walid M. Hassen, Houman Moteshareis (spore culture), René St-Onge (AFM). Funding acquisition, supervising, reviewing: Azam F. Tayabali, Jan J. Dubowski. All authors have read and agreed to the published version of the manuscript.

Conflicts of interest

There are no conflicts to declare.

Data availability

The data supporting this article are provided in Supplementary information†.

Acknowledgements

This work was supported through a grant from Canadian Safety and Security Program of Defence Research and Development Canada, Centre for Security Science (CSSP-2018-P-2342) to Dubowski and Tayabali and subcontract No HT282-183831/001/SV to Dubowski; and the Natural Sciences and Engineering Research Council of Canada (NSERC) discovery grant RGPIN-2020-05558 (JJD).

References

1. P. Bhalla and N. Singh, *The European Physical Journal B*, 2016, **89**, 1-8.
2. J. Goode, J. Rushworth and P. Millner, *Langmuir*, 2015, **31**, 6267-6276.
3. J. Chawich, W. M. Hassen, C. Elie-Caille, T. Lebouis and J. J. Dubowski, *Biosensors*, 2021, **11**, 1450. DOI: 10.1039/D4SD00367E
4. T. Hianik, V. Ostatná, M. Sonlajtnerova and I. Grman, *Bioelectrochemistry*, 2007, **70**, 127-133.
5. Y. Qu, T. Wei, W. Zhan, C. Hu, L. Cao, Q. Yu and H. Chen, *Journal of Materials Chemistry B*, 2017, **5**, 444-453.
6. S. Brosel-Oliu, R. Ferreira, N. Uria, N. Abramova, R. Gargallo, F.-X. Muñoz-Pascual and A. Bratov, *Sensors and Actuators B: Chemical*, 2018, **255**, 2988-2995.
7. J.-H. Park, J.-Y. Byun, H. Mun, W.-B. Shim, Y.-B. Shin, T. Li and M.-G. Kim, *Biosensors and Bioelectronics*, 2014, **59**, 321-327.
8. A. Shalabney and I. Abdulhalim, *Laser Photonics Rev*, 2011, **5**, 571-606.
9. C. S. Zhu, J. Li and H. Wang, *Bio-protocol*, 2023, **13**.
10. Y. Lian, F. He, H. Wang and F. Tong, *Biosensors and Bioelectronics*, 2015, **65**, 314-319.
11. E. Yuhana Ariffin, L. Y. Heng, L. L. Tan, N. H. Abd Karim and S. A. Hasbullah, *Sensors*, 2020, **20**, 1279.
12. X. Xu, X. Lin, L. Wang, Y. Ma, T. Sun and X. Bian, *Biosensors*, 2023, **13**, 868.
13. A. Okamoto and A. Okutani, in *Molecular Medical Microbiology* ed. M. Y. H. Yi-Wei Tang, Dongyou Liu, Andrew Sails, Paul Spearman, Jing-Ren Zhang, Elsevier, Academic Press, Third Edition edn., 2024, DOI: 10.1016/B978-0-12-818619-0.00152-0, ch. 47, pp. 957-986.
14. P. E. Granum and T. Lund, *FEMS microbiology letters*, 1997, **157**, 223-228.
15. H. Moteshareie, W. M. Hassen, Y. Dirieh, E. Groulx, J. J. Dubowski and A. F. Tayabali, *Microorganisms*, 2022, **10**, 1408.
16. S. Riedel, 2005.
17. S. Jöhler, E. M. Kalbhenn, N. Heini, P. Brodmann, S. Gautsch, M. Bağcıoğlu, M. Contzen, R. Stephan and M. Ehling-Schulz, *Frontiers in microbiology*, 2018, **9**, 1915.
18. L. N. Cella, P. Sanchez, W. Zhong, N. V. Myung, W. Chen and A. Mulchandani, *Analytical chemistry*, 2010, **82**, 2042-2047.
19. Y. Wu, C.-W. Wang, D. Wang and N. Wei, *ACS synthetic biology*, 2021, **10**, 333-344.
20. M. M. Lubran, *Annals of Clinical & Laboratory Science*, 1988, **18**, 58-71.
21. E. Nazemi, S. Aithal, W. M. Hassen, E. H. Frost and J. J. Dubowski, *Sensors and Actuators B: Chemical*, 2015, **207**, 556-562.
22. M. R. Aziziyan, W. M. Hassen, D. Morris, E. H. Frost and J. J. Dubowski, *Biointerphases*, 2016, **11**.
23. M. Aziziyan, W. Hassen, H. Sharma, E. S. Sani, N. Annabi, E. Frost and J. Dubowski, *Sensors and Actuators B: Chemical*, 2020, **304**, 127007.
24. M. A. Islam, W. M. Hassen, A. F. Tayabali and J. J. Dubowski, *Biochemical Engineering Journal*, 2020, **154**, 107435.
25. M. A. Islam, W. M. Hassen, A. F. Tayabali and J. J. Dubowski, *ACS omega*, 2021, **6**, 1299-1308.
26. M. A. Islam, W. M. Hassen, I. Ishika, A. F. Tayabali and J. J. Dubowski, *Biosensors*, 2022, **12**, 105.
27. I. Ishika, W. M. Hassen, H. Moteshareie, A. F. Tayabali and J. J. Dubowski, San Francisco, 2023.
28. S. Aithal, N. Liu and J. J. Dubowski, *Journal of Physics D: Applied Physics*, 2016, **50**, 035106.



ARTICLE

Journal Name

29. M. R. Aziziyan, H. Sharma and J. J. Dubowski, *ACS applied materials & interfaces*, 2019, **11**, 17968-17978.
30. H. Sharma, K. Moumanis and J. J. Dubowski, *The Journal of Physical Chemistry C*, 2016, **120**, 26129-26137.
31. O. Voznyy and J. J. Dubowski, *Langmuir*, 2008, **24**, 13299-13305.
32. R. St-Onge, J. Vermette, W. M. Hassen and J. J. Dubowski, *Applied Physics Letters*, 2021, **118**, 222102.
33. X. Li, P. Xue, H. Wang, H. Li, R. Du, J. Gao, K.-Y. Wong and Y. Qin, *Journal of Materials Chemistry C*, 2024, **12**, 16523-16532.
34. A. N. Chattopadhyay, M. Jiang, J. M. V. Makabenta, J. Park, Y. Geng and V. Rotello, *Biosensors*, 2024, **14**, 360.
35. S. Yoon and J. J. Rossi, *Advanced drug delivery reviews*, 2018, **134**, 22-35.
36. R. St-Onge, M. W. Hassen, H. Moteshareie, A. F. Tayabali and J. J. Dubowski, *physica status solidi (b)*, 2025, 2400567.

View Article Online
DOI: 10.1039/D4SD00367E



Data availability (Ishika et al., Regenerable photonic aptasensor...).

The authors declare that the data supporting the findings of this study are available within the paper and its Supplementary Information file. Should any raw data files be needed in another format they are available from the corresponding author upon reasonable request.

